Analytical expressions of the variable viscosity MHD Couette flow with permeable walls using Homotopy analysis method

V. Ananthaswamy[1,*], C. Gantha lakshmi[2]

[1]Department of Mathematics, The Madura College, Madurai, Tamil Nadu, India

[2]M.phil, Mathematics, the Madura College, Madurai, Tamil Nadu, India

International Journal of Applied Sciences (IJAS)

(ISSN: 2371-0381)

[*]**Corresponding Author:** V. Ananthaswamy

Abstract

In this paper, we investigate first and second law of thermodynamic analysis of variable viscosity hydromagnetic, which has Couette flow with permeable walls. The analytical expressions of the dimensionless velocity and dimensionless temperature are derived by using the Homotopy analysis method. Our analytical expression of the dimensionless velocity is compared with the exact solution and a satisfactory agreement is noted. We also derive the analytical expressions for skin friction coefficient, Nusselt number, Entropy generation rate, Bejan number. The HAM contains the convergence control parameter, so we can easily extend to solve other MHD fluid flow problem in engineering and science.

Keywords: Magnetic field; Variable viscosity; Permeable walls; Entropy generation and Bejan number; Homotopy analysis method.

1. Introduction

The information on energy and power losses in the system is yield by thermodynamic irreversibility in the flow system. Minimization of entropy generation in the flow system gives authority to the parametric optimization of the system operation [1]. Mass conservation equation and the first and second law of thermodynamics are three excellence structure of Thermodynamic analysis [2]. The law of mass conservation explains the substances of mass inside of a system and the first law makes clear that the exchanges of energy from one system to another system and energy conservation. The second law describes quantitative relation of the irreversibility of a system through entropy generation, the greater degree of irreversibility, and the more energy consumption. Entropy generation demolish the available energy in the system. It is important in the system of industrial and engineering like Magnetohydrodynamic (MHD) micro-pumps, MHD marine propulsion, MHD lubrication, etc., in the performance of thermal-fluid devices, the entropy generation minimization technique is elevated. A magnetohydrodynamic (MHD) phenomenon accesses to the outcome of mutual interaction between magnetic field and electrically conducting fluid flowing across it. Since the pioneering work of Bejan [3 & 4] on entropy generation minimization on engineering systems, considerable research studies have been carried out to examine entropy generation fluid flows for various applications [5]. The second law for MHD induction devices, such as electromagnetic pumps, and electrical generators are investigated [6]. The entropy generation due to free convection in a

IJAS vol 1, issue 2, AN03, Feb 2016, ISSN: 2371-0381

porous cavity in the presence of magnetic field inspected analytically. Ibanez et. al [8] considered a stationary buoyant MHD flow of a liquid metal immersed in a MHD flow through a vertical rectangular duct. They obtained the optimum conductance ratio of the wall in which the entropy generation is minimized. Eegunjobi et. al [9] were considered the effect of navier slip on entropy generation in a porous channel with suction/injection and investigate entropy generation rate in a thermal system under different physical situation. Makinde et. al [10] were described the effect of Newtonian heating on entropy generation rate in a channel with permeable walls. The model equations are obtained in Theuri, Makinde [11] and solved analytically using Homotopy analysis method. We can apply Homotopy analysis method (HAM) to achieve our objective, which was first developed by Liao [12-20] for general non-linear problems.

2. Mathematical formulation of the problem

Consider the unsteady, incompressible, laminar flow of an electrically conducting variable viscosity fluid between a fixed permeable lower plate and a moving permeable upper plate. The fluid is acted upon by a constant pressure gradient and an external uniform magnetic field is applied perpendicular to the plates as illustrated in figure1. It is presumed that the fluid is injected uniformly into the channel at the lower plate whereas the uniform fluid suction occurs at the moving upper plate. A transverse magnetic field with strength B_0 is applied parallel to the y-axis. There is no applied voltage and the magnetic Reynolds number is small, hence the induced magnetic field and Hall effects are negligible.

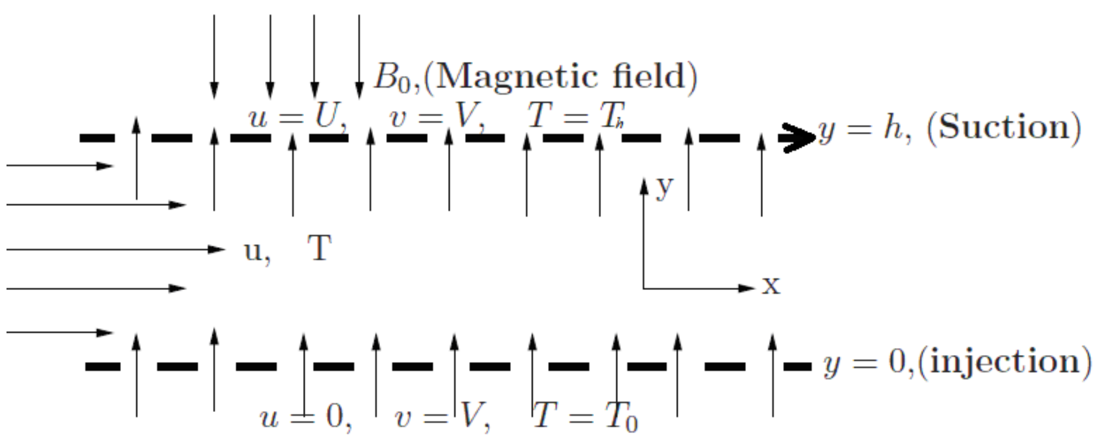

Fig.1: Schematic diagram of the problem

Under these assumptions, the governing equations for the momentum and energy balance in one dimension can be written as follows [5-10]

IJAS vol 1, issue 2, AN03, Feb 2016, ISSN: 2371-0381

$$\frac{\partial u}{\partial t}+V\frac{\partial u}{\partial y}=-\frac{1}{\rho}\frac{\partial P}{\partial x}+\frac{1}{\rho}\frac{\partial}{\partial y}\left(\bar{\mu}(T)\frac{\partial u}{\partial y}\right)-\frac{\sigma B_0{}^2 u}{\rho} \quad (1)$$

$$\frac{\partial T}{\partial t}+V\frac{\partial T}{\partial y}=\alpha\frac{\partial^2 T}{\partial y^2}+\frac{\bar{\mu}(T)}{\rho c_P}\left(\frac{\partial u}{\partial y}\right)^2+\frac{\sigma B_0{}^2 u^2}{\rho c_P} \quad (2)$$

The boundary conditions are:

$$u(y,0)=0, T(y,0)=0 \quad (3a)$$

$$u(0,t)=0, T(0,t)=T_0 \quad (3b)$$

$$u(h,t)=U, T(h,t)=T_h \quad (3c)$$

Here is the channel width, u is the velocity of the fluid, t is the time, P is the fluid pressure, V is the uniform suction / injection velocity at the channel walls, U is the uniform velocity of the upper wall, α is the thermal diffusivity, ρ is the fluid density, σ is the fluid electrical conductivity, k is the thermal conductivity coefficient, C_p is the specific heat at constantpressure,t is the fluid temperature, T_0 is the lower stationary wall temperature and T_0 is the upper wall temperature. The temperature dependent viscosity $\bar{\mu}$ can be expressed as

$$\bar{\mu}(T)=\mu_0 e^{-m(T-T_0)} \quad (4)$$

Where m is a viscosity variation parameter and μ_0 is the fluid dynamic viscosity at the lower fixed wall. Using (1) and (3b), the constant axial pressure gradient will be given as

$$-\frac{1}{\rho}\frac{\partial P}{\partial x}=\frac{\sigma B_0{}^2}{\rho} \quad (5)$$

The eqns. (1) and (2) then becomes

$$\frac{\partial u}{\partial t}+V\frac{\partial u}{\partial y}=\frac{1}{\rho}\frac{\partial}{\partial y}\left(\bar{\mu}(T)\frac{\partial u}{\partial y}\right)-\frac{\sigma B_0{}^2(u-U)}{\rho} \quad (6)$$

$$\frac{\partial T}{\partial t}+V\frac{\partial T}{\partial y}=\alpha\frac{\partial^2 T}{\partial y^2}+\frac{\bar{\mu}(T)}{\rho c_P}\left(\frac{\partial u}{\partial y}\right)^2+\frac{\sigma B_0{}^2(u-U)^2}{\rho c_P} \quad (7)$$

We introduce the following non-dimensional quantities:

$$\tau=\frac{tV}{h},\eta=\frac{y}{h},\alpha=\frac{k}{\rho c_P},w=\frac{u}{U},\theta=\frac{T-T_0}{T_h-T_0},P=\frac{ph}{\mu_0 U},\mu=\frac{\mu}{\mu_0},v=\frac{\mu_0}{\rho} \quad (8)$$

Substituting equation (8) into the equations (6)-(7), we obtain:

$$\mathrm{Re}\, e^{\varepsilon\theta}\frac{\partial w}{\partial \tau}=\frac{\partial^2 w}{\partial \eta^2}-\varepsilon\frac{\partial \theta}{\partial \eta}\frac{\partial w}{\partial \eta}-e^{\varepsilon\theta}\left(\mathrm{Re}\frac{\partial w}{\partial \eta}+Ha(w-1)\right) \tag{9}$$

$$\Pr \mathrm{Re}\frac{\partial \theta}{\partial \tau}=\frac{\partial^2 \theta}{\partial \eta^2}-\mathrm{Re}\Pr\frac{\partial \theta}{\partial \eta}+Ec\Pr e^{-\varepsilon\theta}\left(\frac{\partial w}{\partial \eta}\right)^2+Ec\Pr\left(Ha(w-1)^2\right) \tag{10}$$

With

$$\left.\begin{aligned} &w(\eta,0)=0,\ \theta(\eta,0)=0,\\ &w(0,\tau)=0,\theta(0,\tau)=0,\\ &w(1,\tau)=1,\theta(1,\tau)=1, \end{aligned}\right\} \tag{11}$$

Here,

$$\left.\begin{aligned} &\mathrm{Re}=\frac{V\,h}{v}\\ &pr=\frac{v}{\alpha}\\ &Ec=\frac{U^2}{c_p\,(T_h-T_0)}\\ &Ha=\frac{\sigma\, B_0{}^2\, h^2}{\mu_0}\\ &\varepsilon=m\,(T_h-T_0) \end{aligned}\right\} \tag{12}$$

Where Re, pr, Ec, Ha, ε denote the Reynolds number, Prandtl number, Eckert number, Magnetic field parameter, Viscosity exponent respectively.

Other important physical quantities of interest in this problem are the Skin friction coefficient C_f and Nusselt number Nu, which are defined as:

$$C_f=\frac{h\,\tau_w}{\mu_0 U},\quad Nu=\frac{q_w\,h}{k\,(T_h-T_0)} \tag{13}$$

Where the skin friction τ_w , heat flux q_w at the channel walls are given by

$$\tau_w=\bar{\mu}(T)\left.\frac{\partial u}{\partial y}\right|_{\eta=0,1},q_w=-k\left.\frac{\partial T}{\partial y}\right|_{y=0,1} \tag{14}$$

Substituting the eqn. (14) into an eqn.(13), we obtain

$$C_f=e^{-\varepsilon\theta}\left.\frac{\partial w}{\partial \eta}\right|_{\eta=0,1},\quad Nu=\left.\frac{\partial \theta}{\partial \eta}\right|_{\eta=0,1} \tag{15}$$

IJAS vol 1, issue 2, AN03, Feb 2016, ISSN: 2371-0381

For a given set of parameter values, the reactive third grade flow evolves in time until a steady state condition is attained. Whenever this happens, then the eqns. (8)-(11) becomes,

$$\frac{d^2w}{d\eta^2}-\varepsilon\frac{d\theta}{d\eta}\frac{dw}{d\eta}-e^{\varepsilon\theta}\left(\mathrm{Re}\frac{dw}{d\eta}+Ha\,(w-1)\right)=0 \tag{16}$$

$$\frac{d^2\theta}{d\eta^2}-\mathrm{Re}\,\mathrm{Pr}\frac{d\theta}{d\eta}+Ec\,\mathrm{Pr}\,e^{-\varepsilon\theta}\left(\frac{dw}{d\eta}\right)^2+Ec\,\mathrm{Pr}\,Ha\,(w-1)^2=0 \tag{17}$$

With

$$\left.\begin{array}{l} w(0)=0,\theta(0)=0,\\ w(1)=1,\theta(1)=1,\end{array}\right\} \tag{18}$$

It is important to note that $\varepsilon=0$ corresponds to the case of constant viscosity conducting fluid. The exact solution of equation (1) for the fluid velocity is possible under this constant viscosity scenario and we obtain

$$w(\eta)=1+\frac{e^{a\eta+b}-e^{b\eta+a}}{e^a-e^b} \tag{19}$$

Where $a=\left(\mathrm{Re}+\sqrt{\mathrm{Re}^2+4Ha}\right)/2$ and $b=\left(\mathrm{Re}-\sqrt{\mathrm{Re}^2+4Ha}\right)/2$ equations (16)-(18) represent a nonlinear boundary value.

Other quantities of interest are the skin friction coefficient C_f, Nusselt number Nu, Entropy generation rate Ns and the Bejan number Be which are given as,

$$N_s=\left(\frac{\partial\theta}{\partial\eta}\right)^2+\frac{Br}{\Omega}\left[e^{-\varepsilon\theta}\left(\frac{\partial w}{\partial\eta}\right)^2+Ha\;(w-1)^2\right] \tag{20}$$

Where the temperature difference parameter is $\Omega=(T_h-T_0)/T_0$ and $Br=Ec\ \mathrm{Pr}$ is the Brinkman number. The Bejan number Be is define as

$$Be=\frac{N_1}{N_2}=\frac{1}{1+\Phi}$$

(21)

Where $Ns=N_1+N_2$,

$$N_1=\left(\frac{\partial\theta}{\partial\eta}\right)^2,N_2=\frac{Br}{\Omega}\left[e^{-\varepsilon\theta}\left(\frac{\partial w}{\partial\eta}\right)^2+Ha\;(w-1)^2\right],\Phi=\frac{N_2}{N_1} \tag{22}$$

IJAS vol 1, issue 2, AN03, Feb 2016, ISSN: 2371-0381

It is very important to note that N_1 represents the thermodynamic irreversibility due to heat transfer while N_2 corresponds to the combined effects of fluid friction and magnetic field irreversibility.

3. Solution of the non-linear boundary value problems using the Homotopy analysis method

HAM is a non perturbative analytical method for obtaining series solutions to nonlinear equations and has been successfully applied to numerous problems in science and engineering [11-32]. In comparison with other perturbative and non perturbative analytical methods, HAM offers the ability to adjust and control the convergence of a solution via the so-called convergence-control parameter. Because of this, HAM has proved to be the most effective method for obtaining analytical solutions to highly non-linear differential equations. Previous applications of HAM have mainly focused on non-linear differential equations in which the non-linearity is a polynomial in terms of the unknown function and its derivatives. As seen in (16,17), the non-linearity present in electrohydrodynamic flow takes the form of a rational function, and thus, poses a greater challenge with respect to finding approximate solutions analytically. Our results show that even in this case, HAM yields excellent results.

Liao [12-20] proposed a powerful analytical method for non-linear problems, namely the Homotopy analysis method. This method provides an analytical solution in terms of an infinite power series. However, there is a practical need to evaluate this solution and to obtain numerical values from the infinite power series. In order to investigate the accuracy of the Homotopy analysis method (HAM) solution with a finite number of terms, the system of differential equations were solved. The Homotopy analysis method is a good technique comparing to another perturbation method. The Homotopy analysis method contains the auxiliary parameter h, which provides us with a simple way to adjust and control the convergence region of solution series. Using this method, we can obtain the following solution to (16) and (17) (see Appendix B).

The approximate analytical solution of the eqns. (16) and (17) by using HAM are given by,

$$w(\eta)=\frac{-Ha\,\eta^2}{2}+\left(1+\frac{Ha}{2}\right)\eta-h\left(\begin{array}{l}\dfrac{k_1\eta^3}{6}+\dfrac{k_2\eta^4}{12}+\dfrac{k_3\eta^5}{20}+\dfrac{k_4\eta^6}{30}+\dfrac{k_5\eta^2}{2}\\ -\left(\dfrac{k_1}{6}+\dfrac{k_2}{12}+\dfrac{k_3}{20}+\dfrac{k_4}{30}+\dfrac{k_5}{2}\right)\eta\end{array}\right) \tag{23}$$

$$\theta(\eta)=\left[\begin{array}{l}\frac{-Ec\Pr Ha\eta^2}{2}+\left(1+\frac{Ec\Pr Ha}{2}\right)\eta \\ \qquad -h\left(\frac{l_1\eta^3}{6}+\frac{l_2\eta^4}{12}+\frac{l_3\eta^5}{20}+\frac{l_4\eta^6}{30}+\frac{l_5\eta^2}{2}-\left(\frac{l_1}{6}+\frac{l_2}{12}+\frac{l_3}{20}+\frac{l_4}{30}+\frac{l_5}{2}\right)\eta\right)\end{array}\right] \quad (24)$$

$$C_f=e^{-\varepsilon\theta}\left(-Ha\eta+\left(1+\frac{Ha}{2}\right)-h\left(\begin{array}{l}k_1\frac{\eta^2}{2}+k_2\frac{\eta^3}{3}+k_3\frac{\eta^4}{4}+k_4\frac{\eta^5}{5}+k_5\eta \\ -\left(\frac{k_1}{6}+\frac{k_2}{12}+\frac{k_3}{20}+\frac{k_4}{30}+\frac{k_5}{2}\right)\end{array}\right)\right) \quad (25)$$

$$Nu=-Ec\Pr Ha\eta+\left(1+\frac{Ec\Pr Ha}{2}\right)-h\left(\begin{array}{l}l_1\frac{\eta^2}{2}+l_2\frac{\eta^3}{3}+l_3\frac{\eta^4}{4}+l_4\frac{\eta^5}{5}+l_5\eta \\ -\left(\frac{l_1}{6}+\frac{l_2}{12}+\frac{l_3}{20}+\frac{l_4}{30}+\frac{l_5}{2}\right)\end{array}\right) \quad (26)$$

$$\begin{aligned}Ns=&\left(-Ec\Pr Ha\eta+\left(1+\frac{Ec\Pr Ha}{2}\right)-h\left(\begin{array}{l}l_1\frac{\eta^2}{2}+l_2\frac{\eta^3}{3}+l_3\frac{\eta^4}{4}+l_4\frac{\eta^5}{5}+l_5\eta \\ -\left(\frac{l_1}{6}+\frac{l_2}{12}+\frac{l_3}{20}+\frac{l_4}{30}+\frac{l_5}{2}\right)\end{array}\right)\right)^2 \\ &+\frac{Br}{\Omega}\left[e^{-\varepsilon\theta}\left(-Ha\eta+\left(1+\frac{Ha}{2}\right)-h\left(\begin{array}{l}k_1\frac{\eta^2}{2}+k_2\frac{\eta^3}{3}+k_3\frac{\eta^4}{4} \\ +k_4\frac{\eta^5}{5}+k_5\eta \\ -\left(\frac{k_1}{6}+\frac{k_2}{12}+\frac{k_3}{20}+\frac{k_4}{30}+\frac{k_5}{2}\right)\end{array}\right)\right)^2+Ha\,(w-1)^2\right]\end{aligned} \quad (27)$$

$$N_1=\left(-Ec\Pr Ha\eta+\left(1+\frac{Ec\Pr Ha}{2}\right)-h\left(\begin{array}{l}l_1\frac{\eta^2}{2}+l_2\frac{\eta^3}{3}+l_3\frac{\eta^4}{4}+l_4\frac{\eta^5}{5}+l_5\eta \\ -\left(\frac{l_1}{6}+\frac{l_2}{12}+\frac{l_3}{20}+\frac{l_4}{30}+\frac{l_5}{2}\right)\end{array}\right)\right)^2 \quad (28)$$

$$Be=\frac{N_1}{Ns} \quad (29)$$

Where

$$k_1 = \left(\begin{array}{c} \left(-\varepsilon Ec \Pr Ha^2\right) - \left(\varepsilon Ec \Pr Ha\right) - \varepsilon Ha - \mathrm{Re}\, Ha + Ha\left(1+\frac{Ha}{2}\right) + \varepsilon \mathrm{Re} \\ + \left(\varepsilon \mathrm{Re}\, Ec \Pr \frac{Ha}{2}\right) + \varepsilon \mathrm{Re} \frac{Ha}{2} - \left(\varepsilon \mathrm{Re}\, Ec \Pr \frac{Ha^2}{2}\right) - \left(1 + Ec \Pr \frac{Ha}{2}\right)\varepsilon Ha \end{array} \right) \tag{30}$$

$$k_2 = \left(\begin{array}{c} \left(\varepsilon Ec \Pr Ha^2\right) - \frac{Ha^2}{2} - \varepsilon \mathrm{Re}\, Ha - \left(\varepsilon \mathrm{Re}\ Ec\ \Pr \frac{Ha^2}{2}\right) - \left(\varepsilon \mathrm{Re}\ Ec\ \Pr \frac{Ha}{2}\right) + \varepsilon\ Ha + \varepsilon \frac{Ha^2}{2} \\ - \left(\varepsilon\ \mathrm{Re}\ Ec\ \Pr \frac{Ha^2}{2}\right) + \left(\varepsilon\ Ec\ \Pr \frac{Ha^2}{2}\right) + \left(\varepsilon\ Ec\ \Pr \frac{Ha^2}{2}\right) + \left(\varepsilon\ Ec\ \Pr \frac{Ha^3}{4}\right) \end{array} \right) \tag{31}$$

$$k_3 = \left(\varepsilon \mathrm{Re}\ Ec\ \Pr \frac{Ha^2}{2}\right) + \left(\varepsilon Ec \Pr \frac{Ha^2}{2}\right) - \left(\varepsilon\ Ec \Pr \frac{Ha^3}{4}\right) - \varepsilon \frac{Ha^2}{2} - \left(\varepsilon\ Ec \Pr \frac{Ha^3}{4}\right) \tag{32}$$

$$k_4 = \varepsilon \mathrm{Re}\ Ec \Pr\ Ha^3 \tag{33}$$

$$k_5 = \mathrm{Re}\left(1 + \frac{Ha}{2}\right) + \varepsilon\left(1 + \frac{Ha}{2} + Ec\ \Pr \frac{Ha}{2} + Ec\ \Pr \frac{Ha^2}{4}\right) \tag{34}$$

$$l_1 = \left(\begin{array}{c} \left(-\mathrm{Re}\ Ec \Pr^2 Ha\right) + 2 Ec \Pr\ Ha + Ec \Pr\ Ha^2 + \varepsilon Ec\ \Pr + \left(\varepsilon Ec\ \Pr \frac{Ha^2}{4}\right) \\ + \left(\varepsilon Ec\ \Pr\ Ha\right) + \left(\varepsilon Ec^2 \Pr^2 \frac{Ha}{2}\right) + \left(\varepsilon Ec^2 \Pr^2 \frac{Ha^3}{8}\right) \\ + \left(\varepsilon Ec^2 \Pr^2 \frac{Ha^2}{2}\right) + 2 Ec \Pr Ha + Ec \Pr Ha^2 \end{array} \right) \tag{35}$$

$$l_2 = \left(\begin{array}{c} - Ec \Pr Ha^2 - \left(\varepsilon Ec^2 \Pr^2 \frac{Ha}{2}\right) - \left(\varepsilon Ec^2 \Pr^2 \frac{Ha^3}{8}\right) - \left(\varepsilon Ec^2 \Pr^2 \frac{Ha^2}{2}\right) \\ - \left(2\ \varepsilon Ec \Pr Ha\right) + \varepsilon Ec \Pr Ha^2 - \left(2 Ec^2 \Pr^2 \frac{Ha^2}{2}\right) - \left(\varepsilon Ec^2 \Pr^2 \frac{Ha^3}{2}\right) \\ - Ec \Pr Ha - Ec \Pr Ha^3 - 3 Ec \Pr Ha^2 \end{array} \right) \tag{36}$$

$$l_3 = \left(\begin{array}{c} \left(2\ \varepsilon Ec^2 \Pr^2 \frac{Ha^2}{2}\right) + \left(\varepsilon Ec^2 \Pr^2 \frac{Ha^3}{2}\right) + \varepsilon Ec \Pr Ha^2 \\ + \left(\varepsilon Ec^2 \Pr^2 \frac{Ha^3}{2}\right) + 2\ Ha + 2 \frac{Ha^2}{2} \end{array} \right) \tag{37}$$

$$l_4 = \left(-\varepsilon Ec^2 \Pr^2 \frac{Ha^3}{2} \right) - Ec \Pr \frac{Ha^3}{4} \quad (38)$$

$$l_5 = \text{Re} \Pr + \left(\text{Re}\ Ec \Pr^2 \frac{Ha}{2} \right) - Ec \Pr - Ec \Pr Ha \quad (39)$$

4. Results and Discussion

In this paper, we discuss about the dimensionless fluid velocity, dimensionless fluid temperature, Skin friction coefficient, Nusselt number, Entropy generation rate, Bejan number using Homotopy Analysis Method. Figure 2 represents the Dimensionless transverse coordinate versus Dimensionless fluid velocity. From Figure2 (a), it is clear that when Viscosity Exponent increases the corresponding dimensionless fluid velocity profiles decreases in some fixed values of the other parameters $\text{Re}, Ec, \Pr, Ha$ *and* h and Figure 2(b), it is inferred that when the Magnetic field parameter increases the corresponding dimensionless fluid velocity profiles increases in some fixed values of the other parameters. In Figure 2(c), it is observed that when the Reynolds number increases the corresponding dimensionless fluid velocity profiles decreases in some fixed values of the other parameters.

Figure 3 represent the dimensionless transverse coordinate versus Dimensionless fluid temperature profiles. From Figure 3(a) it is noted that when the magnetic field parameter increases the corresponding dimensionless fluid temperature profiles increases in some fixed values of the other parameters $\text{Re}, Ec, \Pr, \varepsilon$ *and* h and from figure 3(b) it is observed that when the Reynolds number increases the Dimensionless fluid temperature profiles decreases. In Figure 3(c) it is noted that when prandtl number increases the Dimensionless fluid temperature profiles increases. From Figure 3(d) it is inferred that the Eckert number increases the dimensionless fluid temperature profiles increases.

Figure 4 represent the Reynolds number versus Skin friction coefficient. From Figure 4(a) it is clear that when the magnetic field parameter increases the corresponding Skin friction coefficient increases in some fixed values of the other parameters $Ec, \Pr, \varepsilon, \eta = 0$ *and* h and from Figure 4(b) it is inferred that when the Viscosity exponent increases the Skin friction coefficient decreases. In Figure 4(c) it is observed that when magnetic field parameter increases the Skin friction coefficient decreases in some fixed values of the other parameters

$Ec, \Pr, \varepsilon, \eta = 1 \, and \; h$. From Figure 4(d) it is noted that the magnetic field parameter increases the Skin friction coefficient decreases.

Figure 5 represents the Reynolds number versus Nusselt number. Figure 5(a) it is observed that when Magnetic field parameter increases the corresponding Nusselt number increases in some fixed values of the dimensionless parameters $\Pr, Ec, \varepsilon, \eta = 0.$ Figure 5(b) it is clear that when Variable viscosity increases the corresponding Nusselt number decreases. Figure 5(c) it is noted that when Magnetic field parameter increases the corresponding Nusselt number decreases in some fixed values of the dimensionless parameters $\Pr, Ec, \varepsilon, \eta = 1.$ Figure 5(d) it is clear that when Variable viscosity increases the corresponding Nusselt number increases.

Figure 6 represent the Entropy generation rate versus dimensionless transverse coordinate. From Figure 6(a) it is inferred that when the magnetic field parameter increases the corresponding Entropy generation rate increases in some fixed values of the other parameters $Ec, \Pr, \varepsilon, \mathrm{Re}, Br\Omega^{-1} \; and \; h$ and from figure 6(b) it is clear that when the Reynolds number increases the Entropy generation rate decreases. In Figure 6(c) it is observed that when $Br\Omega^{-1}$ increases the Entropy generation rate increases. From Figure 6(d) it is noted that the Viscosity exponent increases the Entropy generation rate decreases.

Figure 7 represent the dimensionless transverse coordinate versus Bejan number. From Figure 7(a) it is noted that when the Magnetic field parameter increases the corresponding Bejan number increases in some fixed values of the other parameters $Ec, \Pr, \mathrm{Re}, Br\Omega^{-1} \; and \; h$ and from figure 7(b) it is inferred that when the Reynolds number increases the Bejan number decreases. In Figure 7(c) it is observed that when $Br\Omega^{-1}$ increases the Bejan number decreases. From Figure 7(d) it is clear that the Viscosity exponent increases the Entropy generation rate decreases. The Table.1 represents the comparison between the exact solution and the HAM solution for the velocity profiles at Viscosity exponent value is zero.

(a)

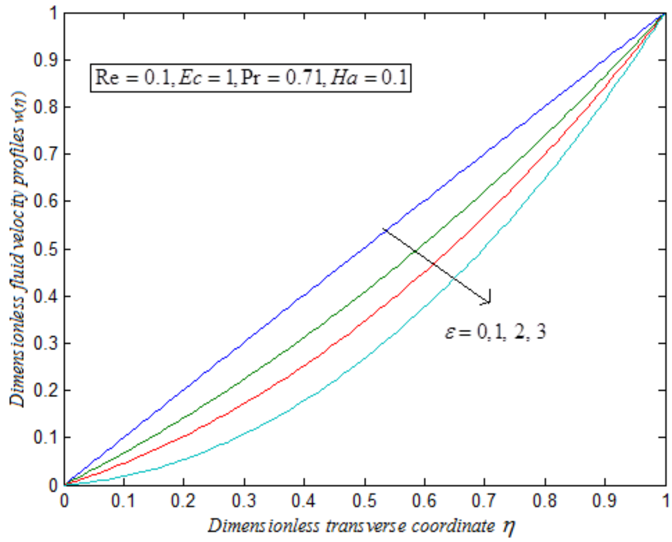

(b)

(c

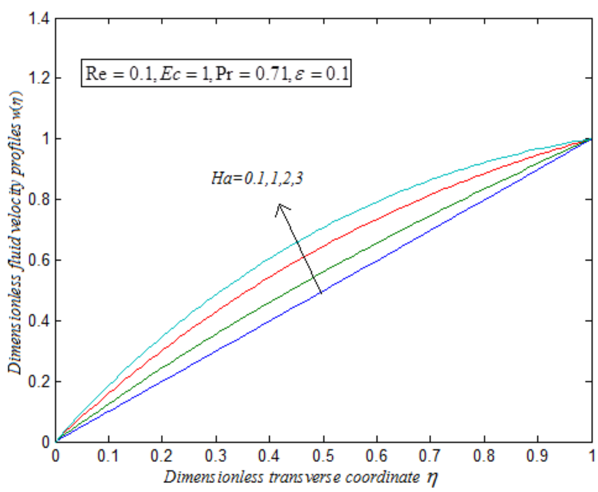

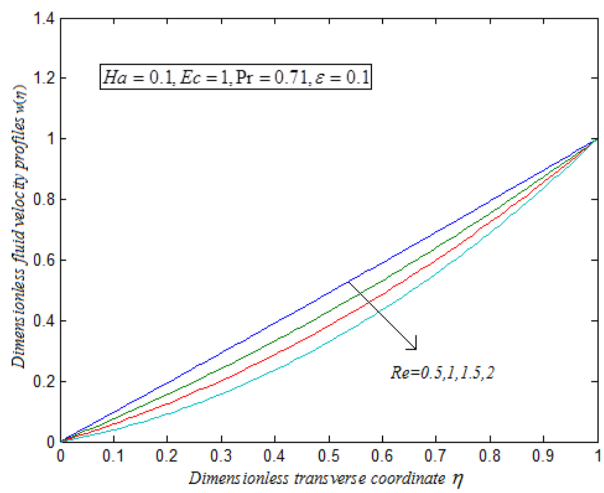

Fig.2: Dimensionless fluid velocity profiles $w(\eta)$ versus dimensionless transverse coordinate (η). The curves are plotted using the eqn. (23) for various values of the dimensionless parameter ε, Ha, Re and in some fixed values of the other dimensionless parameters, when (a) $\mathrm{Re} = 0.1, Ha = 0.1, \mathrm{Pr} = 0.71, Ec = 1, h = -0.51417$. When (b) $\varepsilon = 0.1$, $Ec = 1, \mathrm{Re} = 0.1, \mathrm{Pr} = 0.71$, $h = -0.51417$. When(c) $\varepsilon = 0.1, Ec = 1, \mathrm{Pr} = 0.71, Ha = 0.1, h = -0.51417$.

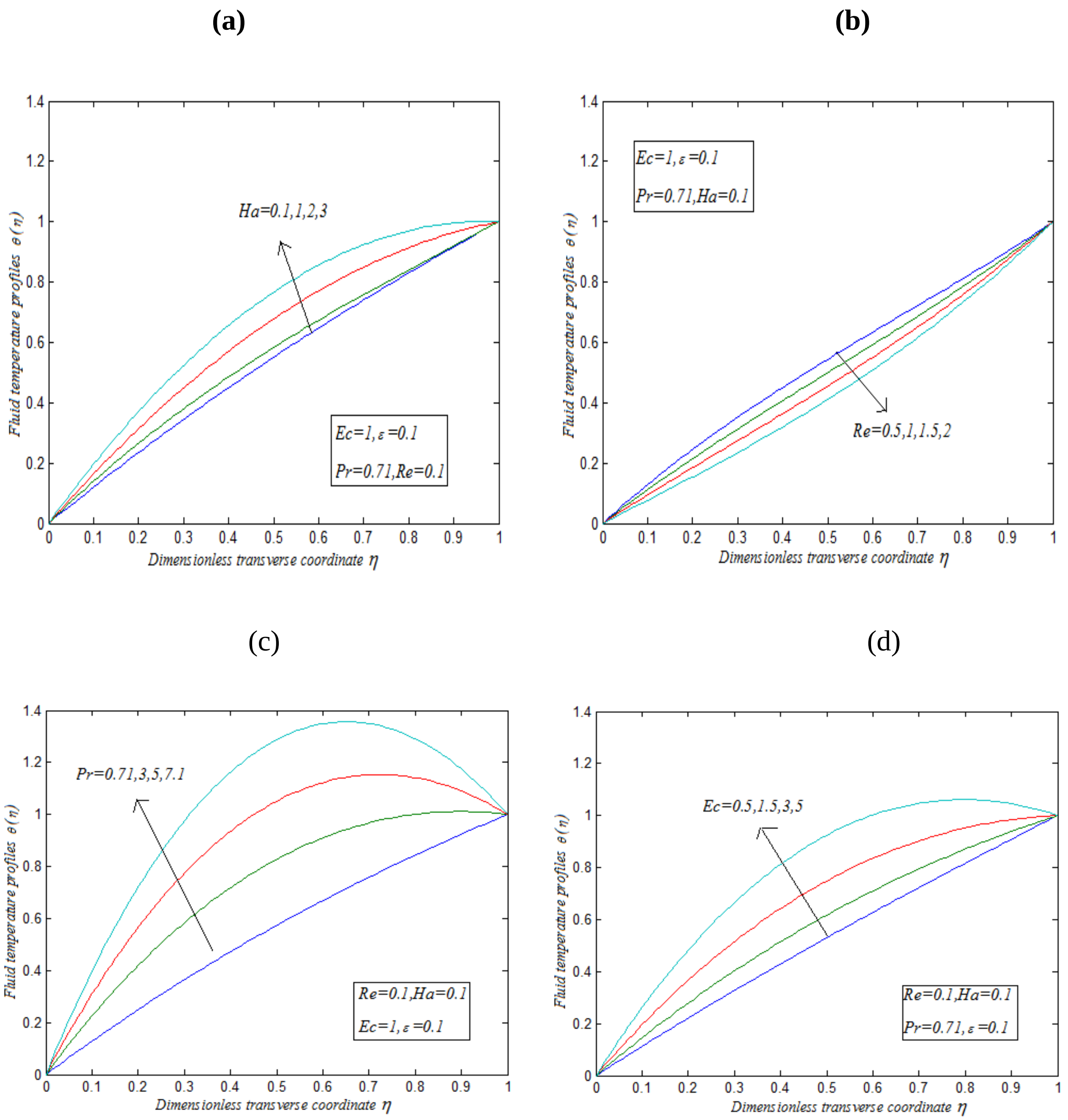

Fig.2: Dimensionless fluid temperature profiles $\theta(\eta)$ versus dimensionless transverse coordinate (η). The curves are plotted using the eqn (24) for various values of the dimensionless parameters $Ha, \mathrm{Re}, \mathrm{Pr}, Ec$ and some fixed values of the parameter when (a) $Ec = 1, \mathrm{Pr} = 0.71,$ $\mathrm{Re} = 0.1, \varepsilon = 0.1, h = -0.83134$. When (b) $Ec = 1, \mathrm{Pr} = 0.71, Ha = 0.1, \varepsilon = 0.1,$ $h = -0.83134$

When (c) $Ec=1,\ Ha=0.1,\ \mathrm{Re}=0.1,\ \varepsilon=0.1, h=-0.83134$. when (d) $Ha=0.1,$ $\mathrm{Pr}=0.71, \mathrm{Re}=0.1, \varepsilon=0.1, h=-0.83134$.

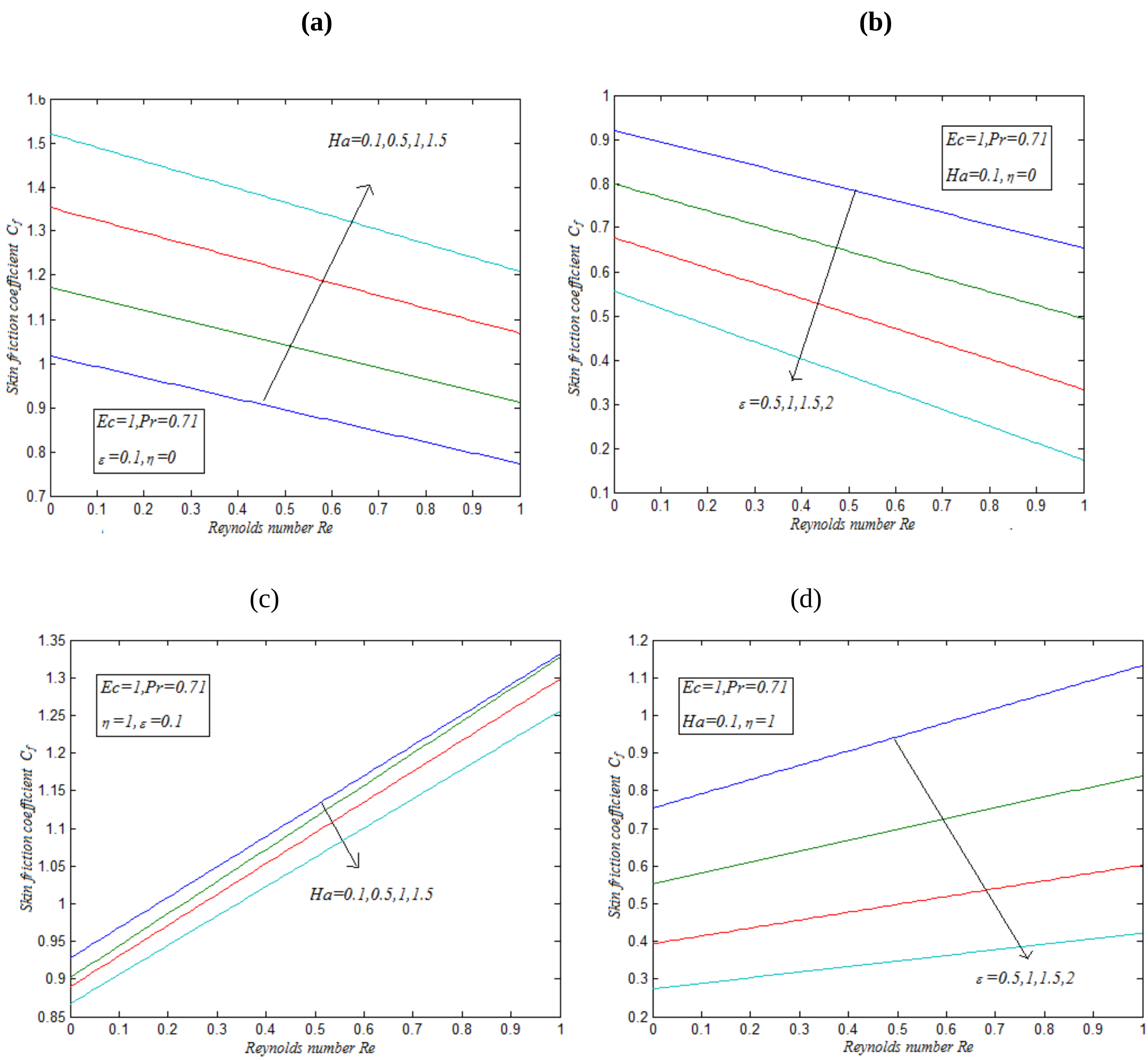

Fig.4: Skin friction coefficient (C_f) versus Reynolds number *(Re)*. The curves are plotted using the eqn (25) for various values of the dimensionless parameter Ha, ε and some fixed values when (a) $Ec=1,\ \mathrm{Pr}=0.71,\ \varepsilon=0.1, \eta=0, h=-0.69375$. when (b) $Ec=1, \mathrm{Pr}=0.71, Ha=0.1,$

$\eta = 0$, $h = -0.69375$. When (c) $Ec = 1, \Pr = 0.71$, $\varepsilon = 0.1$, $\eta = 1, h = -0.69375$. when (d) $Ec = 1$, $\Pr = 0.71$, $Ha = 0.1$, $\eta = 1, h = -0.69375$.

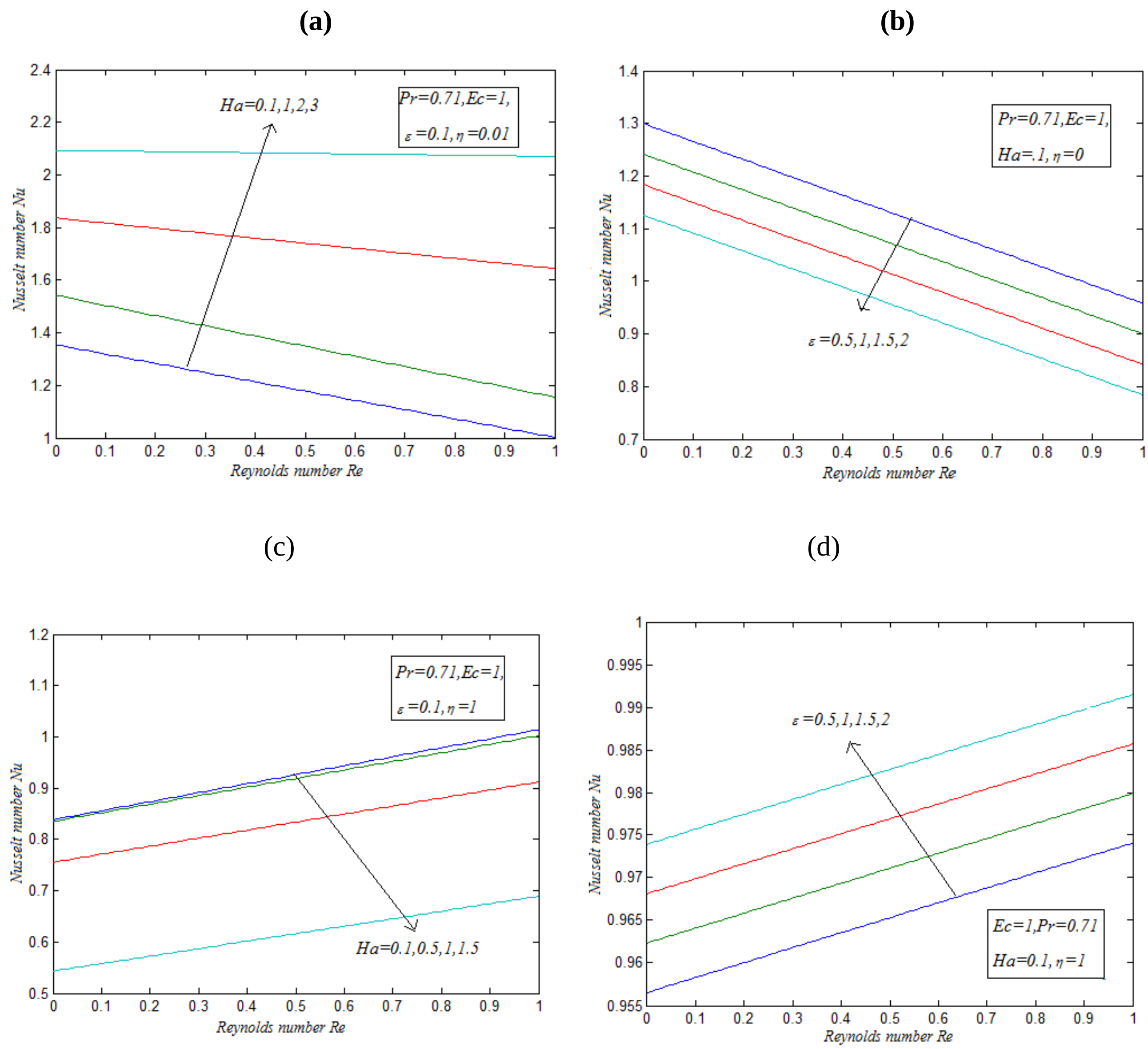

Fig.5: Nusselt number *(Nu)* versus Reynolds number *(Re)* the curves are plotted using the eqn (26) for various values of the dimensionless parameter Ha, ε and some fixed values of the parameter when (a) $Ec = 1, \Pr = 0.71, \varepsilon = 0.1, \eta = 0, h = -0.53125$. when (b) $Ha = 0.1, Ec = 1$, $\Pr = 0.71, \eta = 0, h = -0.53125$. when (c) $Ec = 1, \Pr = 0.71, \varepsilon = 0.1, \eta = 1$, $h = -0.53125$ (d) $Ha = 0.1, Ec = 1, \Pr = 0.71, \eta = 1, h = -0.53125$.

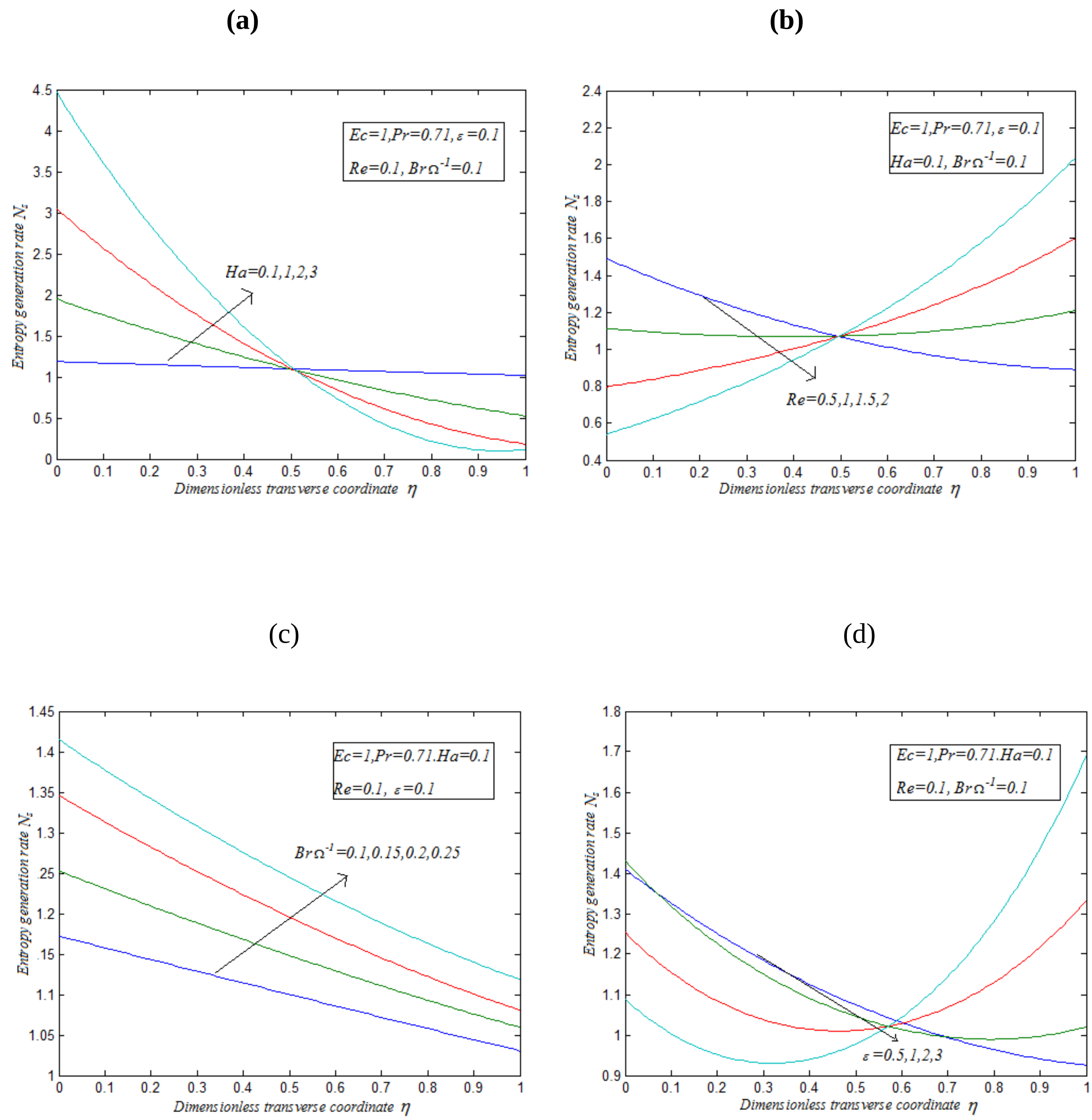

Fig.6: Entropy generation rate*(Ns)* versus dimensionless transverse coordinate (η). The curves are plotted using the eqn (27) for various values of the dimensionless parameter $Ha, \mathrm{Re}, Br\Omega^{-1}, \varepsilon$ and for some fixed values of the parameter when (a) $Br\Omega^{-1} = 0.1$, $\varepsilon = 0.1, Ec = 1, \mathrm{Pr} = 0.71,$, $\mathrm{Re} = 0.1, h = -0.36597$. When (b) $Ha = 0.1, \varepsilon = 0.1, Br\Omega^{-1} = 0.1, Ec = 1$

IJAS vol 1, issue 2, AN03, Feb 2016, ISSN: 2371-0381

$\Pr = 0.71, h = -0.36597$. When (c) $\mathrm{Re} = 0.1, \varepsilon = 0.1, Ec = 1, \Pr = 0.71, Ha = 0.1, h = -0.36597.$ when (d) $Br\Omega^{-1} = 0.1, \mathrm{Re} = 0.1, Ec = 1, \Pr = 0.71, Ha = 0.1, h = -0.36597.$

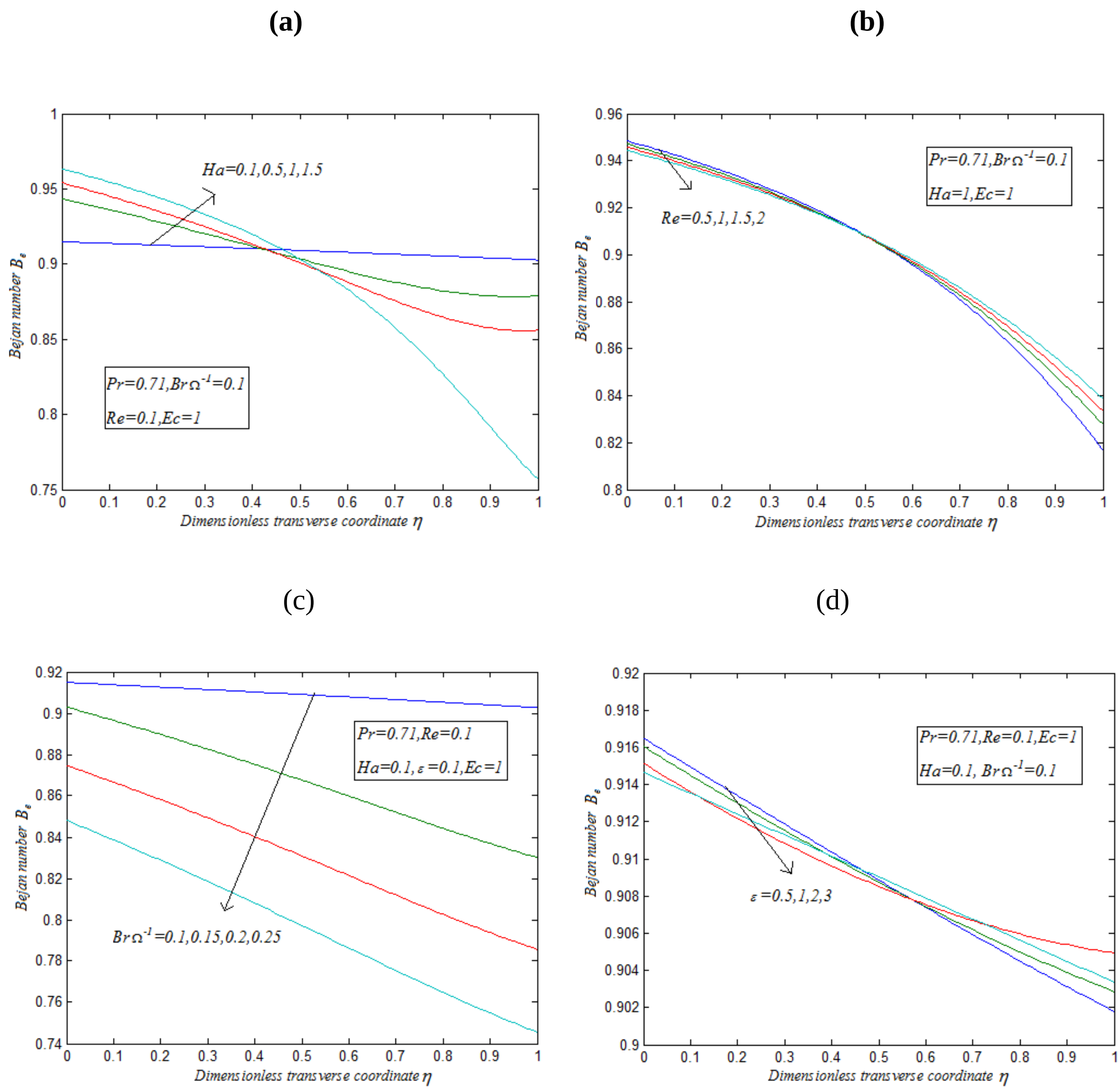

Fig.7: Bejan number (Be) versus dimensionless transverse coordinate (η). The curves are plotted using the eqn (27-29) for various values of the dimensionless parameter $Ha, \mathrm{Re}, \varepsilon, Br\Omega^{-1}$ and some fixed values of the parameter. When (a) $Br\Omega^{-1} = 0.1$, $Ec = 1$, $\Pr = 0.71$, $\mathrm{Re} = 0.1$, $h = -0.21844$. When (b) $Ha = 1, Br\Omega^{-1} = 0.1, \Pr = 0.71, Ec = 1, h = -0.21844$. When (c) $\mathrm{Re} = 0.1$,

IJAS vol 1, issue 2, AN03, Feb 2016, ISSN: 2371-0381

$\Pr = 0.71, Ha = 0.1, Ec = 1, \varepsilon = 0.1, h = -0.21844$. When (d) $Br\Omega^{-1} = 0.1, \Pr = 0.71, \mathrm{Re} = 0.1$ $Ha = 0.1$ and $h = -0.21844$.

Table.1: This table showing the comparison of the exact and HAM solution of dimensionless fluid velocity profile for $\mathrm{Re} = 1, Ha = 1, \varepsilon = 0, \Pr = 0.71$.

η	*Exact solution* ($w(\eta)$)	*HAM solution* ($w(\eta)$) *h= -0.9144*
0	0	0
0.1	0.0881	0.0881
0.2	0.1759	0.1759
0.3	0.2642	0.2642
0.4	0.3541	0.3541
0.5	0.4467	0.4467
0.6	0.5431	0.5431
0.7	0.6449	0.6449
0.8	0.7537	0.753
0.9	0.8713	0.87
1.0	1	1

5. Conclusion

In this paper, the analytical expressions of fluid velocity and temperature profiles were obtained using Homotopy analysis method. Graphical results are presented to analyze the effects of various thermophysical parameters on the velocity and temperature profiles, as well as the entropy generation rate and Bejan number, Nusselt number. The effect of heat transfer considered with permeable wall and Navier slip on entropy generation between two parallel plates. The Homotopy analysis method is a simple and promising method to solve various strongly non-linear differential equations in the area of physical, chemical and biological sciences.

IJAS vol 1, issue 2, AN03, Feb 2016, ISSN: 2371-0381

Acknowledgement

Researchers express their gratitude to the Secretary Shri. S. Natanagopal, Madura College Board, Madurai, Dr. K. M. Rajasekaran, The Principal and Dr. S. Muthukumar, Head of the Department, Department of Mathematics, The Madura College, Madurai, Tamilnadu, India for their constant support and encouragement.

References:

[1] S. Paoletti, F. Rispoli, E. Sciubba, calculation of exergetic losses in compact heat exchanger passages, ASMEAES, 10 (1980): 21-29.

[2]L.C. Wood, Thermodynamics of Fluid Systems,*Oxford University Press*, Oxford, (1975).

[3]A. Bejan,Entropy Generation through heat and fluidflow, New York, USA,2(1982).

[4]A.Bejan Advanced Engineering Thermodynamics,Wiley, USA,(1988).

[5] A.E. Jery,N.Hidouri, M. Magherbi, A.B. Brahim, Effect of an external oriented magnetic field on entropy generation in natural convection, *Entropy*, 12(2010): 1391-1417.

[6] H. Salas,S.Cuevas, M.L.Haro, Entropy generation analysis of magnetohydrodynamic inductiondevices, *J. Phys D: Appl Phys*. 32(1999):2605–2608

[7] S. Mahmud, R.A. Fraser, Magnetohydrodynamic free convection and entropy generation in a square porous cavity, *Int. J. Heat Mass Transfer*, 47(2004): 3245–3256.

[8]G. Ibanez,S.Cuevas, Optimum wall conductance ratio in magnetoconvective flow in a long verticalrectangular duct, *Int. J. Thermal Sci.*, 47 (2008): 1012–1019.

[9]A.S.Eegunjobi, O.D.Makinde, Effects of Navier slip on entropy generation in a porous channel with suction/injection.*Journal of Thermal Science and Technology*, 7(4) (2012): 522 – 535.

[10]O.D.Makinde, A.S. Eegunjobi, Effects of convective heating on entropy generation rate in a channel with permeable walls. *Entropy* 15(2013): 220-233.

[11]D. Theuri, O. D. Makinde, Thermodynamic analysis of variable viscosity MHD unsteady generalized Couette flow with permeable walls, *science publishing group*,3(1),(2014) : 1-8.

[12] S. J. Liao, The proposed homotopy analysis technique for the solution of non linear problems, *Ph.D.Thesis*, Shanghai Jiao Tong University, 1992.

[13]S. J. Liao, An approximate solution technique which does not depend upon small parameters: a special example, *Int. J. Non-Linear Mech*. 30 (1995): 371-380.

[14]S. J. Liao, *Beyond perturbation introduction to the Homotopy analysis method*, 1st edn., Chapman and Hall, CRC press, Boca Raton 67, 2003:336.

[15] S. J. Liao, On the Homotopy analysis method for nonlinear problems, *Appl. Math. Comput*., 147 (2004): 499-513.

[16] S. J. Liao, An optimal Homotopy-analysis approach for strongly nonlinear differential equations,*Commun. Nonlinear Sci. Numer.Simulat.*, 15 (2010): 2003-2016.

[17] S. J. Liao, *The Homotopy analysis method in nonlinear differential equations*, Springer and Higher education press, 2012.

[18] S. J. Liao, An explicit totally analytic approximation of Blasius viscous flow problems. *Int J Nonlinear Mech.*, 34 (1999): 759–78.

[19] S. J. Liao, On the analytic solution of magnetohydrodynamic flows non-Newtonian fluids over a stretching sheet. *J Fluid Mech*., 488 (2003): 189–212.

[20] S. J. Liao, A new branch of boundary layer flows over a permeable stretching plate. *Int J Nonlinear Mech*., 42 (2007): 819–830.

[21] G. Domairry, H. Bararnia, An approximation of the analytical solution of some nonlinear heat transfer equations: a survey by using Homotopy analysis method, *Adv. Studies Theor. Phys.*, 2 (2008): 507-518.

[22] Y.Tan, H.Xu, S.J.Liao, Explicit series solution of travelling waves with a front of Fisher equation. *Chaos Solitons Fractals*., 31(2007): 462–472.

[23] S.Abbasbandy, Soliton solutions for the FitzhughNagumo equation with the homotopy analysis method. *Applied Mathematical Modeling*,32 (2008):2706–2714.

[24] J.Cheng, S.J.Liao, R.N.Mohapatra, K.Vajravelu, Series solutions of nano boundary layer flows by means of the homotopy analysis method. *J Math Anal Appl*., 343 (2008):233–245.

[25] T.Hayat, Z.Abbas, Heat transfer analysis on MHD flow of a second grade fluid in a channelwith porous medium. *Chaos Solitons Fractals*., 38 (2008): 556–567.

[26] T.Hayat, R.Naz, M.Sajid,On the homotopy solution for Poiseuille flow of a fourth grade fluid. *Commun Nonlinear Sci NumberSimul*.,15 (2010): 581–589.

[27] H. Jafari, C. Chun, S. M. Saeidy, Analytical solution for nonlinear gas dynamic Homotopy analysis method, *Appl. Math*., 4 (2009): 149-154.

[28] M.Subha, V.Ananthaswamy, and L.Rajendran, Analytical solution of non-linear boundary value problem for the electrohydrodynamic flow equation, *International Jouranal*

of Automation and Control Engineering., 3(2),(2014): 48-56.

[29] K.Saravanakumar, V.Ananthaswamy, M.Subha, and L.Rajendran, Analytical Solution of nonlinear boundary value problem for in efficiency of convective straight Fins with temperature-dependent thermal conductivity, *ISRN Thermodynamics*, *Article ID* 282481, (2013): 1-18.

[30]V. Ananthaswamy, M. Subha, Analytical expressions for exothermic explosions in a slab, *International Journal of Research* – Granthaalayah, 1(2), (2014): 22-37.

[31]V. Ananthaswamy, S. Uma Maheswari, Analytical expression for the hydrodynamic fluid flow through a porous medium, *International Journal of Automation and Control Engineering*, 4(2), (2015): 67-76.

[32]V. Ananthaswamy, L. Sahaya Amalraj, Thermal stability analysis of reactive hydromagnetic third-grade fluid using Homotopy analysis method, *International Journal of Modern Mathematical Sciences*, 14 (1), (2016): 25-41.

Appendix A

Basic concepts of the Homotopy analysis method [12-32]

Consider the following differential equation:

$$N[u(t)] = 0 \tag{A.1}$$

Where N is a nonlinear operator, $t$denotes an independent variable, $u(t)$ is an unknown function. For simplicity, we ignore all boundary or initial conditions, which can be treated in the similar way. By means of generalizing the conventional Homotopy method, Liao (2012) constructed the so-called zero-order deformation equation as:

$$(1-p)\,L[\varphi(t;p) - u_0(t)] = ph\,H(t)\;N[\varphi(t;p)] \tag{A.2}$$

where $p \in [0,1]$ is the embedding parameter, $h \neq 0$ is a nonzero auxiliary parameter, $H(t) \neq 0$ is an auxiliary function, L an auxiliary linear operator, $u_0\ (t)$ is an initial guess of $u(t)$, $\varphi(t:p)$ is an unknown function. It is important to note that one has great freedom to choose auxiliary unknowns in HAM. Obviously, when $p = 0$ and $p = 1$, it holds:

$$\varphi(t;0) = u_0(t) \text{ and } \varphi(t;1) = u(t) \tag{A.3}$$

respectively. Thus, as p increases from 0 to 1, the solution $\varphi(t;p)$ varies from the initial guess $u_0(t)$ to the solution $u\ (t)$. Expanding $\varphi(t;p)$ in Taylor series with respect to p, we have:

IJAS vol 1, issue 2, AN03, Feb 2016, ISSN: 2371-0381

$$\varphi(t;p) = u_0(t) + \sum_{m=1}^{+\infty} u_m(t) p^m$$

(A.4)

Where

$$u_m(t) = \frac{1}{m!} \frac{\partial^m \varphi(t;p)}{\partial p^m} \Big|_{p=0} \tag{A.5}$$

If the auxiliary linear operator, the initial guess, the auxiliary parameter *h*, and the auxiliary function are so properly chosen, the series (A.4) converges at *p* =1 then we have:

$$u(t) = u_0(t) + \sum_{m=1}^{+\infty} u_m(t). \tag{A.6}$$

Differentiating (A.2) for *m* times with respect to the embedding parameter *p*, and then setting *p* = 0 and finally dividing them by *m*!, we will have the so-called *mth* -order deformation equation as:

$$L[u_m - \chi_m u_{m-1}] = hH(t)\Re_m(\vec{u}_{m-1}) \tag{A.7}$$

Where

$$\Re_m(\vec{u}_{m-1}) = \frac{1}{(m-1)!} \frac{\partial^{m-1} N[\varphi(t;p)]}{\partial p^{m-1}}$$

(A.8)

and

$$\chi_m = \begin{cases} 0, & m \le 1, \\ 1, & m > 1. \end{cases} \tag{A.9}$$

Applying L^{-1} on both side of equation (A.7), we get

$$u_m(t) = \chi_m u_{m-1}(t) + hL^{-1}[H(t)\Re_m(\vec{u}_{m-1})] \tag{A.10}$$

In this way, it is easily to obtain u_m for $m \ge 1$, at M^{th} order, we have

$$u(t) = \sum_{m=0}^{M} u_m(t) \tag{A.11}$$

When $M \to +\infty$, we get an accurate approximation of the original equation (A.1). For the convergence of the above method we refer the reader to Liao [14]. If equation (A.1) admits unique solution, then this method will produce the unique solution.

IJAS vol 1, issue 2, AN03, Feb 2016, ISSN: 2371-0381

Appendix B

Approximate analytical expressions of the non-linear differential eqns. (16) and (17) using Homotopy analysis method

In this Appendix, we indicate how the eqns. (23) - (24) are derived in this paper. To find the solution of the eqns. (16) and (17) when $\varepsilon\theta$ small, eqns. (16) and (17) reduces to

$$\frac{d^2w}{d\eta^2}-\varepsilon\frac{d\theta}{d\eta}\frac{dw}{d\eta}-(1+\varepsilon\theta)\left(\mathrm{Re}\frac{dw}{d\eta}+Ha(w-1)\right)=0 \tag{B.1}$$

$$\frac{d^2\theta}{d\eta^2}-\mathrm{Re}\,\mathrm{Pr}\frac{d\theta}{d\eta}+Ec\,\mathrm{Pr}(1-\varepsilon\theta)\left(\frac{dw}{d\eta}\right)^2+Ec\,\mathrm{Pr}\,Ha\,(w-1)^2=0 \tag{B.2}$$

We construct the Homotopy analysis method for the eqns (B.1) and (B.2) are as follows:

$$(1-p)\left(\frac{d^2w}{d\eta^2}+Ha\right)-h\,p\left(\begin{array}{l}\frac{d^2w}{d\eta^2}-\varepsilon\frac{d\theta}{d\eta}\frac{dw}{d\eta}-\mathrm{Re}\frac{dw}{d\eta}-Ha\;w+Ha-\varepsilon\theta\,\mathrm{Re}\frac{dw}{d\eta}\\+\varepsilon\theta\,Ha-\varepsilon\theta\,Ha\;w\end{array}\right)=0 \tag{B.3}$$

$$(1-p)\left(\frac{d^2\theta}{d\eta^2}+Ec\,\mathrm{Pr}\,Ha\right)-h\,p\left(\begin{array}{l}\frac{d^2w}{d\eta^2}-\mathrm{Re}\,\mathrm{Pr}\frac{d\theta}{d\eta}+Ec\,\mathrm{Pr}\left(\frac{dw}{d\eta}\right)^2-Ec\,\mathrm{Pr}\,\varepsilon\theta\left(\frac{dw}{d\eta}\right)^2\\+Ec\,\mathrm{Pr}\,Ha\,w^2+Ec\,\mathrm{Pr}\,Ha-2\,Ec\,\mathrm{Pr}\,Ha\,w\end{array}\right)=0 \tag{B.4}$$

The approximate solution of the eqns. (B.3) and (B.4) are as follows:

$$w=w_0+p\,w_1+p^2\,w_2+p^3\,w_3+p^4\,w_4+\cdots\cdots \tag{B.5}$$

$$\theta=\theta_0+p\,\theta_1+p^2\,\theta_2+p^3\,\theta_3+p^4\,\theta_4+\cdots\cdots \tag{B.6}$$

The boundary conditions are as follows:

$$w(0)=0,\theta(0)=0 \tag{B.7}$$

$$w(1)=1,\theta(1)=1 \tag{B.8}$$

Substituting the eqns (B.5) and (B.6) into the eqns (B.3) and (B.4) we get

$$(1-p)\left[\frac{d^2(w_0+pw_1+\cdots)}{d\eta^2}+Ha\right]-h\,p\left[\begin{array}{l}\frac{d^2(w_0+pw_1+\cdots)}{d\eta^2}\\ -\varepsilon\frac{d(\theta_0+p\theta_1+\cdots)}{d\eta}\frac{d(w_0+pw_1+\cdots)}{d\eta}\\ -\mathrm{Re}\frac{d(w_0+pw_1+\cdots)}{d\eta}-Ha(w_0+pw_1+\cdots)\\ +Ha+\varepsilon(\theta_0+p\theta_1+\cdots)Ha\\ -\varepsilon(\theta_0+p\theta_1+\cdots)\mathrm{Re}\frac{d(w_0+pw_1+\cdots)}{d\eta}\\ -\varepsilon(\theta_0+p\theta_1+\cdots)Ha(w_0+pw_1+\cdots)\end{array}\right]=0 \qquad \text{(B.9)}$$

$$(1-p)\left[\begin{array}{l}\frac{d^2(\theta_0+p\theta_1+\cdots)}{d\eta^2}\\ +Ec\Pr Ha\end{array}\right]-h\,p\left[\begin{array}{l}\frac{d^2(\theta_0+p\theta_1+\cdots)}{d\eta^2}-\mathrm{Re}\Pr\frac{d(\theta_0+p\theta_1+\cdots)}{d\eta}\\ +Ec\Pr\left(\frac{d(w_0+pw_1+\cdots)}{d\eta}\right)^2+Ec\Pr Ha\\ -Ec\Pr\varepsilon(\theta_0+p\theta_1+\cdots)\left(\frac{d(w_0+pw_1+\cdots)}{d\eta}\right)^2\\ +Ec\Pr Ha(w_0+pw_1+\cdots)^2\\ -2Ec\Pr Ha(w_0+pw_1+\cdots)\end{array}\right]=0 \qquad \text{(B.10)}$$

Comparing the coefficients of like powers of p in the eqns (B.9) and (B.10) we get,

$$p^0:\frac{d^2w_0}{d\eta}+Ha=0 \qquad \text{(B.11)}$$

$$p^0\ :\frac{d^2\theta_0}{d\eta}+Ec\Pr Ha=0 \qquad \text{(B.12)}$$

$$p^1:\frac{d^2w_1}{d\eta^2}-\frac{d^2w_0}{d\eta^2}-Ha-h\left[\begin{array}{l}\frac{d^2w_0}{d\eta^2}-\varepsilon\frac{d\theta_0}{d\eta}\frac{dw_0}{d\eta}-\mathrm{Re}\frac{dw_0}{d\eta}-Ha\,w_0+Ha\\ -\varepsilon\theta_0\mathrm{Re}\frac{dw_0}{d\eta}-\varepsilon\theta_0 Ha\,w_0+\varepsilon\theta_0 Ha\end{array}\right]=0 \qquad \text{(B.13)}$$

IJAS vol 1, issue 2, AN03, Feb 2016, ISSN: 2371-0381

$$p^1: \frac{d^2\theta_1}{d\eta^2} - \frac{d^2\theta_0}{d\eta^2} - Ec\,\Pr Ha - h\begin{bmatrix} \frac{d^2\theta_0}{d\eta^2} - \operatorname{Re}\Pr\frac{d\theta_0}{d\eta} + Ec\Pr\left(\frac{dw_0}{d\eta}\right)^2 \\ -Ec\Pr\varepsilon\,\theta_0\left(\frac{dw_0}{d\eta}\right)^2 + Ec\Pr Ha \\ +Ec\Pr Ha\,(w_0)^2 - 2\,Ec\Pr Ha\; w_0 \end{bmatrix} = 0 \quad \text{(B.14)}$$

Solving the eqns (B.11)-(B.14) using the boundary conditions (B.7) and (B.8) we can obtain the following results:

$$w_0 = \frac{-Ha\,\eta^2}{2} + \left(1 + \frac{Ha}{2}\right)\eta \quad \text{(B.15)}$$

$$w_1 = -h\left(\frac{k_1\eta^3}{6} + \frac{k_2\eta^4}{12} + \frac{k_3\eta^5}{20} + \frac{k_4\eta^6}{30} + \frac{k_5\eta^2}{2} - \left(\frac{k_1}{6} + \frac{k_2}{12} + \frac{k_3}{20} + \frac{k_4}{30} + \frac{k_5}{2}\right)\eta\right) \quad \text{(B.16)}$$

$$\theta_0 = \frac{-Ec\Pr Ha\,\eta^2}{2} + \left(1 + \frac{Ec\Pr Ha}{2}\right)\eta \quad \text{(B.17)}$$

$$\theta_1 = -h\left(\frac{l_1\eta^3}{6} + \frac{l_2\eta^4}{12} + \frac{l_3\eta^5}{20} + \frac{l_4\eta^6}{30} + \frac{l_5\eta^2}{2} - \left(\frac{l_1}{6} + \frac{l_2}{12} + \frac{l_3}{20} + \frac{l_4}{30} + \frac{l_5}{2}\right)\eta\right) \quad \text{(B.18)}$$

Where $k_1, k_2, k_3, k_4, k_5, l_1, l_2, l_3, l_4, l_5$ are defined in the text eqns (33)-(42) respectively.

According to the HAM, we can conclude that

$$w = \lim_{P\to 1} w(\eta) = w_0 + w_1 \quad \text{(B.19)}$$

$$\theta = \lim_{P\to 1} \theta(\eta) = \theta_0 + \theta_1 \quad \text{(B.20)}$$

After putting (B.15) and (B.16) into (B.19), (B.17) and (B.18) into (B.20) we obtain the solution in the text eqns. (23) and (24).

Appendix: C

Nomenclature

Symbol	Meaning
C_p	Specific heat at a constant pressure
U	Fluid velocity
V	Uniform suction/injection velocity

T	Fluid temperature
Be	Bejan number
H	Channel width
Re	Reynolds number
Br	Brinkmann number
(x, y)	Cartesian coordinates
X	Dimensionless axial coordinate
M	Variable viscosity parameter
K	Thermal conductivity
P	Fluid pressure
Ha	Magnetic field parameter
Pr	Prandtl number
Ec	Eckert number
w	Dimensionless velocity
B_0	Magnetic field strength
α	Thermal diffusivity
θ	Dimensionless temperature
Ω	Temperature difference parameter
η	Dimensionless transverse coordinate
$\overline{\mu}(T)$	Temperature dependent viscosity
μ_0	Fluid viscosity at ambient temperature
μ	Fluid viscosity
ϕ	Irreversibility ratio
ρ	Fluid density
σ	Electrical conductivity